The Planck Scale and Agent Based Simulations of Quantum Spacetime

Ralph Abraham[1],**Sisir Roy**[2,3]

[1] Mathematics Department, University of California, Santa Cruz, CA ,95064 USA

[2]Physics and Applied Mathematics Unit, Indian Statistical Institute, Calcutta-700035, INDIA

[3] College of Science, George Mason University, USA

[1]e-mail: abraham@vismath.org

[2,3]e-mail: sisir@isical.ac.in

Abstract

The macroscopic spacetime (or its underlying mesoscopic or microscopic substratum) has been shown to emerge from a more fundamental concept, a cellular network. A NetLogo model of spacetime that self-organizes from such a microscopic cellular network is described here. This will shed new light on understanding spacetime at the Planck scale.

Keywords : Planck scale, NetLogo , Self-organization, Cellular network

PACS: 05.65 +b, 02.60.-x, 89.75 kd.

1 Introduction

Recent developments in quantum gravity[1] and string theory[2] have raised lot of debates about the very concept of spacetime and causality at Planck scale. The length and time at Planck scale are the smallest length (10^{-33}cm) and smallest time(10^{-43}sec) below which no measurement is possible. The Planck length and Planck time can be expressed as

$$l_p = \sqrt{\bar{h}G/c^3}$$

and

$$t_p = \sqrt{\bar{h}G/c^5}$$

respectively, where $\bar{h}$, G, c are the Planck constant, the gravitational constant, and the speed of light. The very concept of space, time and causality loose their meaning below this scale. The spacetime behaves discretely at Planck scale. The metaphor that Nature behaves discretely at the Planck scale is not at all clear to 21st century scientists. One of the present authors (SR) along with Requardt[3] described how macroscopic spacetime or its underlying mesoscopic substratum emerges from a more fundamental concept, a fluctuating cellular network around the Planck scale. Henceforth, we shall call it the RR model of spacetime after Requardt and Roy. It is generally beleived that no physical laws that are valid in continuum space-time will be valid below or near the Planck scale. RR proposes that geometry emerges from a purely relational picture a la Leibniz. The discrete structure at the Planck scale consists of elementary nodes which interact or exchange information with each other via bonds, playing the role of irreducible elementary interactions.

Essentially, the RR model is a two-level system. The microscopic level, *QX*, is a dynamical cellular network of *nodes* and *bonds*. The macroscopic level, *ST*, that self-organizes from QX is an another cellular network, in which the nodes, or *supernodes*, are the *cliques* (that is, maximal fully connected subgraphs) of a graph, $G(t)$, of the QX level, bound in a network by *superbonds*. The system of [RR] ends with a metric space, but we wish to advance to a macroscopic cellular network embedded in Euclidean space. Even though an isometric embedding is not possible, we will try to approximate one using neural network technology.

First we will model the dynamical cellular network, QX, with its cellular automaton-like dynamics, as described in RR. We introduce an extension of the theory by interpolating one step. Rather than defining the emergent supernodes directly as the cliques of a graph $G(t)$ of QX, we derive from $G(t)$ the permutation graph of a permutation, $P(t)$. We then define the supernodes of the emergent ST as the cliques of the permutation graph of $P(t)$, rather than those of $G(t)$. The purpose of this extension is to achieve a manageable computational task.

Spatial geometry is going to evolve from the dynamics of the QX network. For the emergence of spatial organization we use a neural network approach, based on the differences of finite sets, rather than the random metric of RR based on fuzzy sets. This process is intended as a preliminary step, that eventually will lead to an implementation and simulation of the [RR] scheme. Later, we intend to go on to the emergence of a temporal geometry in a subsequent paper.

2 The QX model

Let $N > 1$ be an integer. We consider a set of N nodes, n_i, $i \in \bar{N} = \{1, \cdots, N\}$. The linear indexing scheme for the nodes is meant as a convenience for programming, and not as a spatial lattice.

2.1 Notations

Nodes have internal node states, $s_i \in q.Z$, where q is a positive real number, the *quantum of information*. For each $i, k \in \bar{N}$, with $i < k$, we have a link or *bond*, b_{ik}, having an internal bond state, $J_{ik} \in \{-1, 0, +1\}$, which might be interpreted as outgoing, off, or incoming, respectively[4,5,6]. In this approach, the bond states are dynamical degrees of freedom which, a fortiori, can be switched off or on. The wiring, the pure geometry of the network, is also an emergent, dynamical property and is not given in advance. Consequently, the nodes and bonds are not arranged in any regular way, e.g., a lattice, and there is no fixed near/far order. This implies geometry will become to some extent a relational (Machian) concept and is not an a priori element of our formalism.

2.2 Local dynamical law

The node and bond states are to be updated in discrete steps of clock time, $t = z.\tau, z \in Z$, and $\tau \in R^+$ is an elementary interval of clock time. While various local dynamical laws might be contemplated, we are going to use just one, which is Definition 2.1 of Requardt and Roy[3]. Assume two critical parameters given, $0 \leq \lambda_1 \leq \lambda_2$. Then these are the rules:

$$s_i(t + \tau) - s_i(t) = q.\Sigma J_{ki}(t) \tag{1}$$

$$J_{ik}(t + \tau) = 0 \; if \; |s_i(t) - s_k(t)| =: |s_{ik}(t)| > \lambda_2 \tag{2}$$

$$J_{ik}(t + \tau) = \pm 1 \; if \; 0 < \pm s_{ik}(t) < \lambda_1 \tag{3}$$

$$J_{ik}(t + \tau) = J_{ik}(t) \; if \; s_{ik}(t) = 0 \tag{4}$$

And if $\lambda_1 \leq \pm s_{ik}(t) \leq \lambda_2$, then,

$$J_{ik}(t + \tau) = \pm 1 \; if \; J_{ik}(t) \neq 0 \; else \; J_{ik}(t + \tau) = 0 \tag{5}$$

Of course, we must have initial conditions, $s_i(0)$ and $J_{ik}(0)$ in order to begin a dynamical trajectory of the cellular network.

2.3 Graphical displays

Our model will begin with random values for the node and bond states, and then evolve with discrete steps of clock time according to the rules above.

Our first display will show the instantaneous state of the bonds of QX. Note that there are no bonds $J_{ik}(t),\ i = k$. Also, our bond states ± 1 may be interpreted as arriving or departing directed links in a directed graph, or *digraph*. Hence $J_{ik}(t),\ i \neq k$ comprise a skew- symmetric matrix, and we need only display the case $i < k$. So our display will be an $N \times N$ upper semi-diagonal matrix of bond trivalues, which we may indicate with the color code, green for $+1$, red for -1, and yellow for 0.

We use the diagonal of the triangular matrix to show the node-states with colors: red, orange, yellow, or green, for decreasing values of node-state, s_i, which is the current charge on the $i - th$ node. Alternatively, we may show the node-weights on the diagonal. This is the number of links at a node in the graph view.

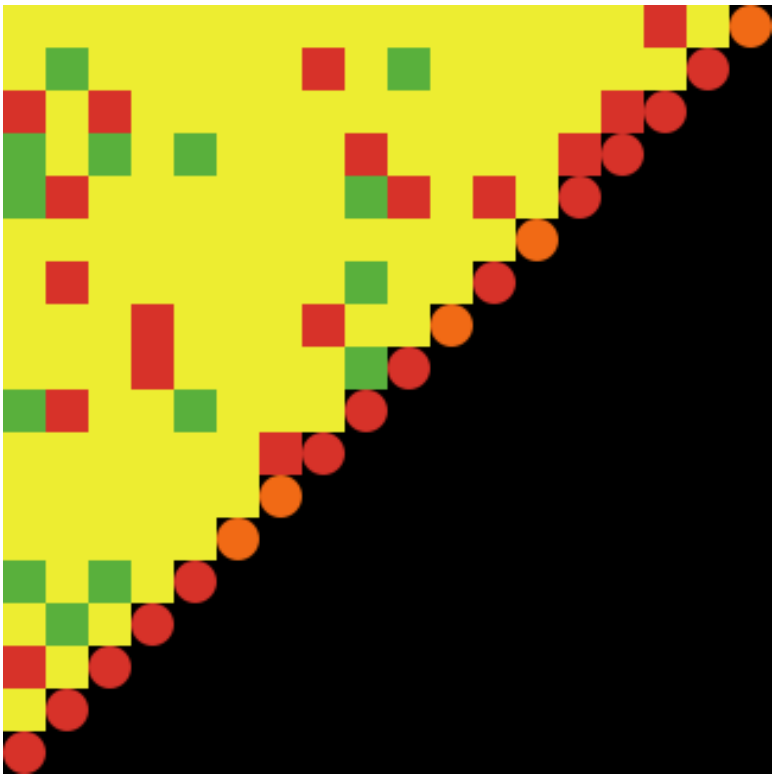

Figure 1: The NetLogo graphics window showing bond-states and node-weights.

A second display shows the node-diffs, or relative potentials, $s_{ik} = s_i - s_k$ in a convenient color

code. Here we are regarding the node-state s_i as a sort of charge density, that increases by a receipt of charge when $J_{ik} = 1$, and decreases when $J_{ik} = -1$.

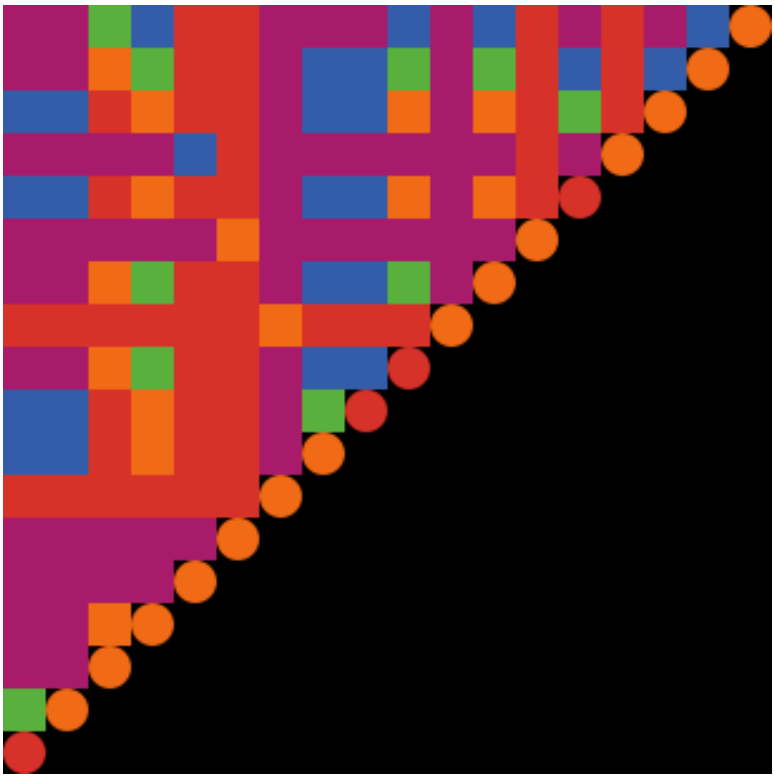

Figure 2: The NetLogo graphics window showing node-diffs and node-weights.

A third display shows the digraph as follows. For any $(i, k), i \neq k$, the corresponding position in the display is illuminated if there is a directed link from the $i - th$ node to the $k - th$.

The fourth and final display is the simple undirected graph underling the digraph, shown as a symmetric matrix.

3 The ST model

The process by which the ST network self-organizes from QX, as described in [RR], uses, as supernodes, the cliques of the graph $G(t)$ that underlies the digraph $D(t)$ of the dynamical cellular network described above. We find this inconvenient as the computation of cliques for a general graph is notoriously difficult[7]. Meanwhile, it is relatively easy to compute the cliques of a permutation graph. So we are going to modify the prescription of Requardt and Roy by the addition of an intermediate step, as follows. The graph G is given to us with an arbitrary ordering of its nodes. So we have a sequence of n nodes, $[Q_0, ..., Q_n]$.

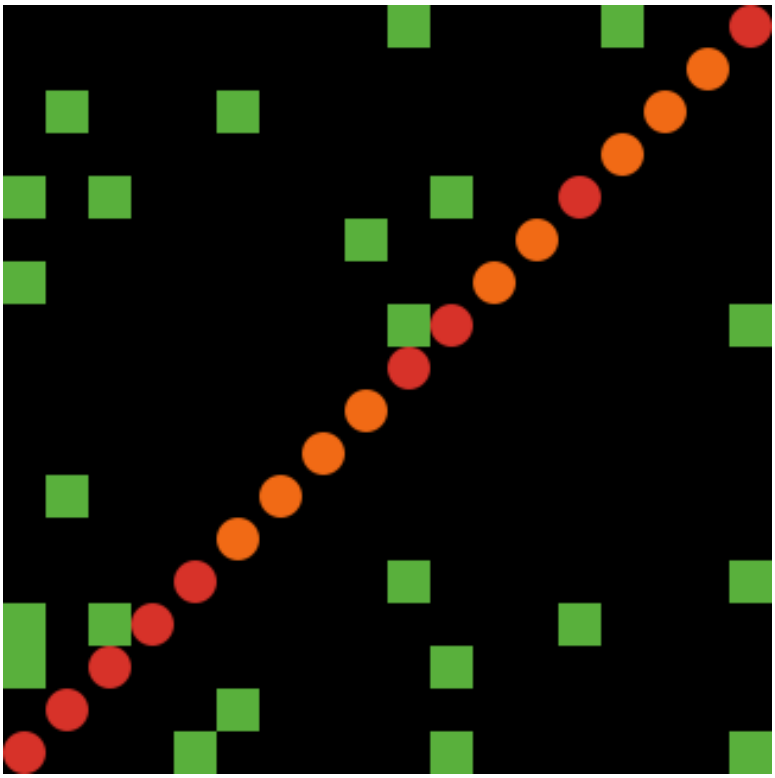

Figure 3: The NetLogo graphics window showing the digraph and node-weights.

3.1 The supernodes

We define the it node-weight of a node as the number of its adjacent nodes, that is, the number of links attached to it. Let w_i denote the weight of the $i-th$ node, Q_i. Next, we form, for the $i-th$, node, the pair (i, w_i), and collect all of these in a sequence of pairs, A. Now we sort this sequence of pairs in order of decreasing weights, obtaining a new sequence of pairs, B. Finally, from B, we extract the sequence of first members, obtaining the n-permutation, P. We may now easily compute the cliques of the permutation graph of P as the supernodes for the ST network.

One may object that the cliques of the graph of P are not intuitively motivated, but we feel that they are at least as meaningful as the cliques of G. In fact, if we were to try to identify the cliques of G by hand, we would probably start with the nodes of highest weight.

Our NetLogo model includes a button "show permutation" that prints out, when pressed at time t, the permutation, $P(t)$. Our intention is to export this to an external program, such as *Combinatorica*, to compute the cliques, and then to submit these to a further NetLogo model (or self-organizing map software) to obtain the ST model.

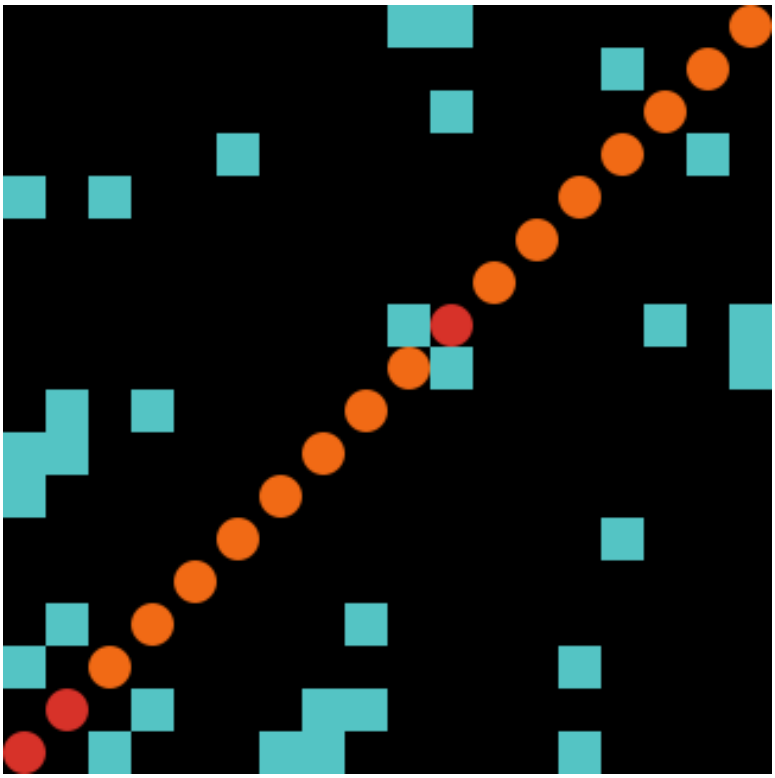

Figure 4: The NetLogo graphics window showing the graph and node-weights.

3.2 The clique computation

The cliques of a permutation graph are just the inverse sequences of its permutation, which may be found by inspection, or by software such as *Combinatorica*. We explain by considering a few examples. Here we will follow [CDM; pp. 69-71] closely, except that we use parentheses rather than brackets for vectors, that is, sequences of natural numbers.

3.2.1 Example 1

Let π be the permutation $(6, 5, 4, 3, 2, 1)$ of the sequence $(1, 2, 3, 4, 5, 6)$. Then the inversion vector of π is the 5-vector $v = (5, 4, 3, 2, 1)$. The permutation graph of π, G_π, consists of the six nodes with a link from i to j only if they are inverted, that is, $i < j$ while $\pi(i) > \pi(j)$. In this case, all nodes of G_π are linked: $6 * 5/2 = 15$ links.

In [CDM], a clique of a graph is a subset of vertices which are totally connected. We say a clique is *maximal-size* if no node may be adjoined without destroying the clique property of total connection. In [RR], a *clique* is always maximal-size, and we shall use this convention throughout. So in this example, there is just one clique: the entire graph is totally connected. The unique clique is the set, $\{1, 2, 3, 4, 5, 6\}$. This is a set of nodes (indices) of G_π, not of values of the permutation, π.

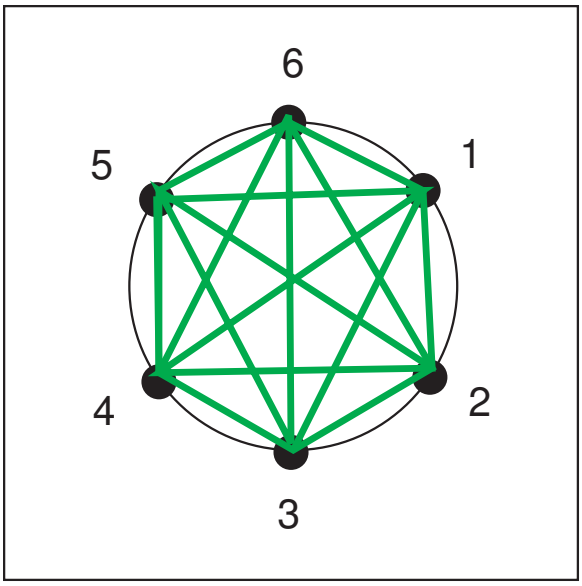

Figure 5: Permutation graph for Example 1 (one clique).

3.2.2 Example 2

Let π be the permutation $(3, 2, 1, 6, 5, 4)$. Then the permutation graph, G_π, has six links, for the inversions: $(1, 2)$ as $\pi(1) = 3 > \pi(2) = 2$, and similarly $(2, 3)$, $(1, 3)$, $(4, 5)$, $(5, 6)$, and $(4, 6)$. There are two cliques, each of the same size, 3, which are disjoint. The permutation graph is the disjoint union of the two cliques, $\{1, 2, 3\}$ and $\{4, 5, 6\}$.

Note that the cliques of G_π correspond to maximal decreasing sequences of π, and these are observable in reading π from left to right. It is easiest to reverse the sequence of π, and read its maximal increasing sequences. In this case, **Reverse**$(\pi) = (4, 5, 6, 1, 2, 3)$ from which we read immediately the two cliques, $\{4, 5, 6\}$ and $\{1, 2, 3\}$

3.2.3 Example 3

Let π be the permutation $(3, 6, 2, 5, 1, 4)$. In this case, **Reverse**$(\pi) = (4, 1, 5, 2, 6, 3)$ from which we read immediately the two cliques, $\{4, 5, 6\}$ and $\{1, 2, 3\}$, as before.

3.2.4 Example 4

Let π be the permutation $(4, 1, 2, 3, 6, 5)$. In this case, **Reverse**$(\pi) = (5, 6, 3, 2, 1, 4)$ from which we read immediately the four cliques, $(5, 6)$, $(3, 4)$,(2,4), $(1, 4)$.

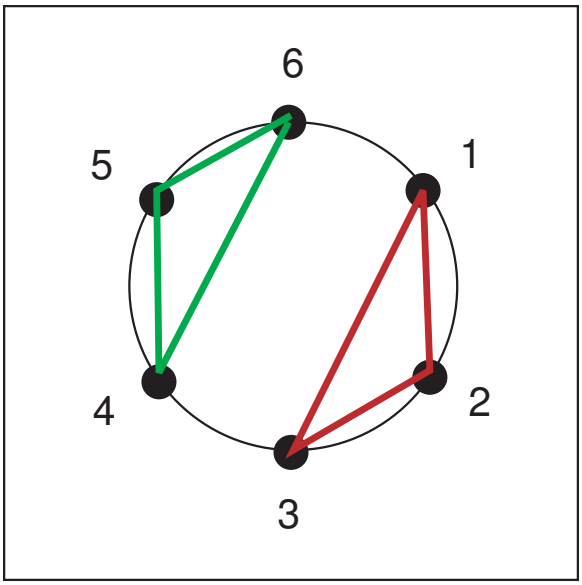

Figure 6: Permutation graph for Example 2 (two cliques).

3.3 The superbonds and weights

Given a permutation arising from our simulation of the QX cellular network, we are going to define its cliques as the nodes of our ST graph. So we now need to connect these clique nodes with links, the *superbonds* of our scheme. It is here that we diverge from RR, and follow our path to precise sets and weights of entanglement, rather than fuzzy sets and random metric distances. We will use Example 4 above to illustrate the concepts.

Given a finite set of natural numbers, S, define its *span* by the set,

$$span(S) = [min(S), \ldots, max(S)],$$

and its *length* as the natural number,

$$length(S) = card(span(S)) = max(S) - min(S) + 1.$$

Note that the empty set has length zero.

Next, given two finite sets of natural numbers, S and T, define their *lap* by the set,

$$lap(S,T) = span(S) \cap span(T),$$

and their *lapsize* by the natural number,

$$lapsize(S,T) = card(lap(S,T)),$$

that is, the cardinality of their lap. Note that if the two sets are disjoint, then their lapsize is zero.

Similarly, we define their *span* by the set,

$$span(S,T) = span(S \cap T),$$

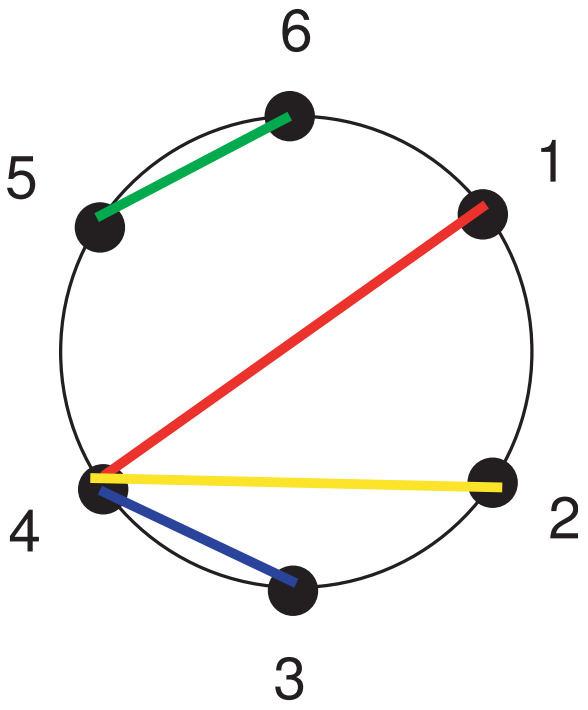

Figure 7: Permutation graph for Example 4 (four cliques).

and their *spansize* by the natural number,

$$spansize(S,T) = card(span(S,T)).$$

Finally, we define the *weight of entanglement* of the pair (S,T) (not both empty) by the ratio,

$$weight(S,T) = 1 - lapsize(S,T)/spansize(S,T).$$

Note that the weight of two sets with disjoint spans is one. Also, if $span(S) = span(T)$, then $weight(S,T) = 0$.

We may wish at this point to modify the definition of weight in the case of two sets with disjoint spans, so that the weight may be greater than one, and actually measure the distance between the two spans.

Now let's compute the weights of pairs of the cliques of Example 4 above. Let $K_1 = (5,6)$, $K_2 = (3,4)$, $K_3 = (2,4)$, and $K_4 = (1,4)$. We will compute the symmetric matrix $W = [w_{ij} = weight(K_i, K_j)]$. Note that all the diagonal elements are zero.

We begin with w_{12}. But this is one as K_1 and K_2 are disjoint. Similarly with w_{13} and w_{14}, so we have only three weights to compute from the definitions. Here we go:

$$w_{23} = weight(K_2, K_3) = 1 - lapsize(K_2, K_3)/spansize)K_2, K_3),$$

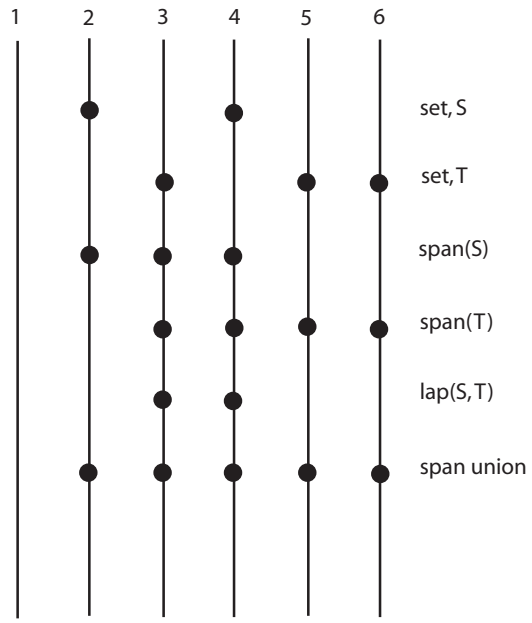

Figure 8: Computation of the weight of entanglement of two sets.

$$lap(K_2, K_3) = span(K_2) \cap span(K_3) = span(\{3,4\}) \cap span(\{2,4\}) = \{3,4\} \cap \{2,3,4\} = \{3,4\}$$
$$lapsize(K_2, K_3) = card(lap(K_2, K_3)) = card(\{3,4\}) = 2$$
$$spansize(K_2, K_3) = card(span(K_2 \cup K_3)) = card(\{2,3,4\}) = 3$$

so finally,

$$w_{23} = 1 - 2/3 = 1/3.$$

Similarly, we compute w_{24},

$$lap(K_2, K_4) = span(K_2) \cap span(K_4) = span(\{3,4\}) \cap span(\{1,4\}) = \{3,4\} \cap \{1,2,3,4\} = \{3,4\}$$
$$lapsize(K_2, K_4) = card(lap(K_2, K_4)) = card(\{3,4\}) = 2$$
$$spansize(K_2, K_4) = card(span(K_2 \cup K_4)) = card(\{1,2,3,4\}) = 4$$

so finally,

$$w_{24} = 1 - 2/4 = 1/2.$$

Finally, we compute w_{34},

$$lap(K_3, K_4) = span(K_3) \cap span(K_4) = span(\{2,4\}) \cap span(\{1,4\}) = \{2,3,4\} \cap \{1,2,3,4\} = \{2,3,4\}$$

$$lapsize(K_3, K_4) = card(lap(K_3, K_4)) = card(\{3,4\}) = 3$$

$$spansize(K_3, K_4) = card(span(K_3 \cup K_4)) = card(\{1,2,3,4\}) = 4$$

so finally,

$$w_{34} = 1 - 3/4 = 1/4.$$

Displaying all our weights in matrix form, we have,

$$\begin{bmatrix} 0 & 1 & 1 & 1 \\ 1 & 0 & 1/3 & 1/2 \\ 1 & 1/3 & 0 & 1/4 \\ 1 & 1/2 & 1/4 & 0 \end{bmatrix}$$

4 The spatial organization

The above simulations are preliminary to the emergence of spatial organisation. In RR framework, the emergence of spatial organization has been formulated as a random metric space[8,9]. Instead, we will seek an isometric embedding of our cliques and their entanglement weights. We now have our cliques and weights, but notice that the triangle inequalities are not satisfied.

4.1 The isometric embedding problem

Even were the distances to satisfy the triangle inequalities, an isometric embedding into a Euclidean space of a given dimension might not be possible. For example, consider the pyramid or tetrahedron, the simplest of the Platonic solids. This is a system of four nodes with all six weights equal. We may isometrically embed in Euclidean 3-space, but not in the plane. As in our case, we may have a cellular system with millions of nodes and wish to embed as isomterically as possible in 3-space or the plane, so we must adjust a random embedding by a dynamical process.

So we propose to regard the nodes and weights as a neural network, and try to embed the nodes in Euclidean space (dimension two or three) such that the distances at least approximate the weights as well as possible. One possible technique for this process is the neural network method of self-organizing maps[10]. A simpler method, easily implemented in NetLogo, is a multidimensional variant of least squares, as follows[11]. Let us begin with a random map of the nodes into Euclidean space. Then, sum up the squares of the differences between the internodal distances and the weights, and integrate the negradient of this sum function to minimize it.

4.2 The method of least squares

We will illustrate this simpler method for the special case described in detail in the preceding section. This case has four nodes. As above, let $w_{12} = w_{13} = w_{14} = 1$, $w_{23} = 1/3$, $w_{24} = 1/2$, and $w_{34} = 1/4$. We are going to try to embed these four nodes in the Euclidean plane, as isometrically as possible. We begin with an arbitrary map of the nodes into the plane, assuming only that all the positions are distinct.

Let $p_i = (x_i, y_i)$ denote the current position of node K_i in the Cartesian plane, $i = 1, 2, 3, 4$, and d_{ij} the Euclidean distance between K_i and K_j. Then there is a contribution $e_{ij} = (d_{ij} - w_{ij})^2$ to the square error we wish to minimize. Let E denote the total error, that is, the sum of the six pair errors, e_{ij}, for pairs $ij = 12, 13, 14, 23, 24, 34$. We regard E as a function of the eight real variables, $(x_1, y_1, ..., x_4, y_4)$. We will adjust the positions so as to minimize this function, that is, to find the most nearly isometric positions. In fact, we will integrate the negradient of E by the Euler algorithm.

So we must now compute symbolically the partial derivatives of E with respect to each of the eight coordinate variables. Note that E is the sum of six square terms. For any one of the eight coordinate variables, there are three of the six square terms that yield zero. For example, the square term involving p_1 and p_2, $e_{12} = (d_{12} - w_{12})^2$, has nonzero partial derivates only with respect to the four variables, x_1, y_1, x_2, y_2.

For example: The partial of e_{12} with respect to x_1 is

$$\partial_{x_1} e_{12} = \partial_{x_1}(d_{12} - w_{12})^2 = 2(d_{12} - w_{12})\partial_{x_1} d_{12}$$

while

$$\partial_{x_1} d_{12} = \partial_{x_1}[(x_1 - x_2)^2 + (y_1 - y_2)^2]^{1/2} = (x_1 - x_2)/d_{12}$$

and thus

$$\partial_{x_1} e_{12} = 2(d_{12} - w_{12})(x_1 - x_2)/d_{12} = 2(1 - w_{12}/d_{12})(x_1 - x_2)$$

as $d_{12} \neq 0$. Note that if $d_{12} = w_{12}$, which is the result we would like, then $\partial_{x_1} e_{12} = 0$. Likewise, if $x_1 = x_2$.

All of the partial differentiations of E with respect to the eight coordinates are very similar to this first case, we must only take care with the signs.

Thus we find the eight new coordinates, $(X_1, ..., Y_4)$, by the Euler algorithm applied to the negradient of the error, E, as follows. For the first of the eight coordinates of the adjusted configuration,

$$X_1 = x_1 - (\partial_{x_1} E)\Delta t$$

where Δt is chosen suitably small. Using the above template for all three nonzero terms,

$$\partial_{x_1} E = \partial_{x_1}(e_{12} + e_{13} + e_{14})$$

we have,

$$X_1 = x_1 - 2\{+(1 - w_{12}/d_{12})(x_1 - x_2) + (1 - w_{13}/d_{13})(x_1 - x_3) + (1 - w_{14}/d_{14})(x_1 - x_4)\}\Delta t$$

The other seven adjusted coordinates are found similarly,

$$Y_1 = y_1 - 2\{+(1 - w_{12}/d_{12})(y_1 - y_2) + (1 - w_{13}/d_{13})(y_1 - y_3) + (1 - w_{14}/d_{14})(y_1 - y_4)\}\Delta t$$

$$X_2 = x_2 - 2\{-(1 - w_{12}/d_{12})(x_1 - x_2) + (1 - w_{23}/d_{23})(x_2 - x_3) + (1 - w_{24}/d_{24})(x_2 - x_4)\}\Delta t$$

$$Y_2 = y_2 - 2\{-(1 - w_{12}/d_{12})(y_1 - y_2) + (1 - w_{23}/d_{23})(y_2 - y_3) + (1 - w_{24}/d_{24})(y_2 - y_4)\}\Delta t$$

$$X_3 = x_3 - 2\{-(1 - w_{13}/d_{13})(x_1 - x_3) - (1 - w_{23}/d_{23})(x_2 - x_3) + (1 - w_{34}/d_{34})(x_3 - x_4)\}\Delta t$$

$$Y_3 = y_3 - 2\{-(1 - w_{13}/d_{13})(y_1 - y_3) - (1 - w_{23}/d_{23})(y_2 - y_3) + (1 - w_{34}/d_{34})(y_3 - y_4)\}\Delta t$$

$$X_4 = x_4 - 2\{-(1 - w_{14}/d_{14})(x_1 - x_4) - (1 - w_{24}/d_{24})(x_2 - x_4) - (1 - w_{34}/d_{34})(x_3 - x_4)\}\Delta t$$

$$Y_4 = y_4 - 2\{-(1 - w_{14}/d_{14})(y_1 - y_4) - (1 - w_{24}/d_{24})(y_2 - y_4) - (1 - w_{34}/d_{34})(y_3 - y_4)\}\Delta t$$

Notice the pattern of signs: $+++, -++, --+, ---$.

5 Possible Implications

The validity of the postulates of geometry has been questioned around or below Planck scale during the development of modern physics in the late twentieth century. It is worth mentioning that Riemann[12] in 1854 discussed similar issues in connection with the validity of metrical relations in indefinitely small regions. Here, we have started with a working hypothesis that a type of cellular network exists at the ultimate level of the universe from which the usual spacetime emerges. On the other hand, the people working on non-commutative geometry[13] started with the proposition that space is pointless and a kind of non-commutativity of algebra exists at the ultimate level. However, they also discussed the concept of fuzzy space at Planck scale. In our present work, we have shown the emergence of spatial organization using agent based simulations. Our goal is to generate spatiotemporal organization i.e. four-dimensional spacetime starting with cellular networks and their evolution. This will shed new light not only on understanding the postulates of geometry at small scale but also the evolution of the universe and the theory of gravity

Acknowledgement : One of the authors (SR) is indebted to CEOSR, College of Science, George Mason University, USA for the support during the last part of this work.

References

1. Isham C.J.(1995) Structural issues in quantum gravity, http://xxx.lanl.gov/gr-qc/9510063

2. Smolin L.(1998) The future of spin networks, in S.A. Hugget et al (eds),*The Geomterical Universe*, Oxford University Press, Oxford.

3. Requardt, Manfred, and Sisir Roy(2001) (Quantum) space-time as a statistical geometry of fuzzy lumps and the connection with random metric spaces, *Classical and Quantum.Grav.* **18**, 3039,

4. Nowotny, Thomas, and Manfred Requardt(1998) Dimension theory on graphs and networks, *Journ.Phys.A*, **31**, 2447.

5. Nowotny, Thomas, and Manfred Requardt(1999) Pregeometric concepts on graphs and cellular networks, http://xxx.lanl.gov/hep-th/9806135.

6. Nowotny, Thomas(2001), Doctoral Dissertation.

7. Pemmeraju, Sriram, and Steven Skiena(2003) *Computational Discrete Mathematics: Combinatorics and Graph Theory wth Mathematica.* Cambridge: Cambrige University Press.

8. Roy, Sisir(1998) *Statistical Geometry and Applications to Microphysics and Cosmology.* Dordrecht; Boston: Kluwer Academic.

9. de Gesu Vito and Roy Sisir(2002) *Lecture Notes in Computer Science.* Vol. 2275, p. 360 (2002).

10. Hagan, Martin T., Howard B. Demuth, and Mark Beale(1996) *Neural Network Design*, PWS Publishing.

11. Gerald, Curtis F.(1970) *Applied Numerical Analysis*, Reading, Mass, Addison-Wesley.

12. Riemann Bernhard(1854) On the Hypotheses Which Lie at the Foundations of Geometry, in *Source Book in Mathematics* ed. Smith David, Dover Publications, New York (1959).

13. Madore J.(1999)*An Introduction to Noncommutative Differential Geometry and its Physical Applications*, Cambridge (England) ; New York : Cambridge University Press, 2nd edition.